

DoA-Aided MMSE Channel Estimation for Wireless Communication Systems

Franz Weißer, Nurettin Turan, and Wolfgang Utschick

TUM School of Computation, Information and Technology, Technical University of Munich, Germany

{franz.weisser, nurettin.turan, utschick}@tum.de

Abstract—This paper investigates the combination of parametric channel estimation with minimum mean square error (MMSE) estimation. We propose a direction-of-arrival (DoA)-aided two-stage channel estimation technique that utilizes the decomposition of wireless communication channels into a line-of-sight (LoS) path and its orthogonal subspace. After estimating the channel along the dominant direction, we utilize a Gaussian mixture model to estimate the conditionally Gaussian distributed random vector, which represents the multipath propagation. The proposed two-stage estimator allows pre-computing the respective estimation filters, tremendously reducing the computational complexity. Numerical simulations with typical channel models depict the superior performance of our proposed two-stage estimation approach compared to state-of-the-art methods.

Index Terms—Channel estimation, DoA estimation, spatial channel model, Gaussian mixture models, machine learning

I. INTRODUCTION

With the need for higher data rates and more reliable transmissions, channel estimation has become a crucial task in modern multiple-input-multiple-output (MIMO) communication systems [1]. Similar to other fields of wireless communication, machine learning-based methods have been introduced for channel estimation [2]–[4]. Based on a representative training data set, machine learning-based methods learn a prior distribution during the learning stage, which enhances the channel estimation performance later on. Notably, the works of [3], [4] propose channel estimation methods that approximate the minimum mean square error (MSE) estimator, focusing on the statistics of the channels without utilizing any structural information given by the geometric channel model.

As an alternative approach, parametric channel estimators have been proposed, which build on the multipath propagation characteristics of wireless channels, e.g., [5], [6]. These so-called model-based techniques have gained relevance in recent years, estimating the parameters of each path and constructing the channel based on these estimates. Those parametric channel estimators are especially relevant when considering joint communication and sensing (JCAS) systems. JCAS systems aim to integrate communication and sensing functionalities in one system to enhance overall capabilities. In [7], a comprehensive overview of the progress in JCAS research is given.

In [5], it is shown that direction-of-arrival (DoA)-based channel estimation can achieve superior performance com-

This work was supported by the Federal Ministry of Education and Research of Germany in the programme of “Souverän. Digital. Vernetzt.”. Joint project 6G-life, project identification number: 16KISK002

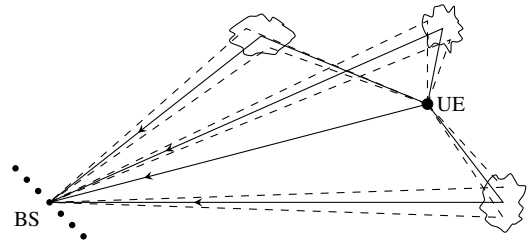


Fig. 1. Illustration of a wireless channel between the user equipment (UE) and the base station (BS) with one LoS path and three scattering clusters.

pared to the linear MMSE (MMSE) estimation, while the authors in [6] evaluate performance bounds, validating the superiority of parametric channel estimation. Notably, these works focus primarily on ray-based channel models, describing each multipath component by a distinct ray stemming from a point scatterer. These models are often assumed for high frequencies. However, for sub 6 GHz, realistic channel models, e.g., [8], model scatterers not as points but rather as point clouds resulting in propagation clusters composed of a dominant path and accompanying subpaths, which may be not resolved by distinct rays. Studies on the impact of subpaths for higher frequencies, such as mmWave are ongoing research, cf. [9]. The estimation of these subpaths is crucial for the communication task since they allow the full utilization of the achievable data rate [10]. In the context of massive MIMO systems, the substantially improved spatial resolution offered by large-scale antenna arrays has led to the employment of spatial channel models [3], [11].

Contributions: This work aims to bridge the gap between parametric and MMSE-based channel estimation. To this end, we reformulate the estimation problem similar to the generalized sidelobe cancellor (GSC) into line-of-sight (LoS) and non-LoS (NLoS) subspaces based on DoA estimates either provided by localization and positioning functionalities or established DoA estimators. Afterwards, we introduce two independent estimators, where the estimation of the NLoS components utilizes the channel estimator based on a Gaussian mixture model (GMM), as proposed in [4]. This combination seeks to enhance the accuracy and efficiency of channel estimation in realistic wireless communication scenarios.

II. SYSTEM MODEL

Let us consider a base station (BS), equipped with M antennas that receives uplink signals from a single-antenna user equipment (UE). We assume the UE is located in the far field, and we have a frequency-flat, block-fading channel. Under the assumption that orthogonal pilots are used, we can correlate the received pilot observations with the transmitted signals, such that only the channel of interest is present in the observations. The received signal vector at the BS can be written as

$$\mathbf{y}(t) = \mathbf{h}(t) + \mathbf{n}(t), \quad t = 1, \dots, T, \quad (1)$$

with the channel vectors $\mathbf{h}(t)$ and the additive white Gaussian noise (AWGN) $\mathbf{n}(t) \sim \mathcal{N}_{\mathbb{C}}(\mathbf{0}, \mathbf{C}_{\mathbf{n}} = \sigma^2 \mathbf{I}_M)$. Additionally, the following Rician model is assumed [8], [12]

$$\mathbf{h}(t) = \sqrt{\frac{KM}{K+1}} \mathbf{a}(\theta) e^{j\phi(t)} + \sqrt{\frac{M}{K+1}} \mathbf{h}_{\text{NLoS}}(t) \quad (2)$$

where K denotes the Rician factor, $\mathbf{a}(\theta)$ and $\phi(t)$ are the steering vector and phase of the dominant path, and \mathbf{h}_{NLoS} denotes the channel corresponding to the scatterers. Each channel is normalized by its path loss. Based on a set of parameters $\boldsymbol{\delta}$, which describe the directions and properties of the clusters, the NLoS channel vectors are considered as conditionally Gaussian distributed [3], [8]

$$\mathbf{h}_{\text{NLoS}}(t) | \boldsymbol{\delta} \sim \mathcal{N}_{\mathbb{C}}(\mathbf{0}, \mathbf{C}_{\text{NLoS}}(\boldsymbol{\delta})). \quad (3)$$

The spatial covariance matrix of the NLoS components is given by

$$\mathbf{C}_{\text{NLoS}}(\boldsymbol{\delta}) = \int_{-\pi}^{\pi} g(\vartheta, \boldsymbol{\delta}) \mathbf{a}(\vartheta) \mathbf{a}^H(\vartheta) d\vartheta, \quad (4)$$

where $g(\vartheta, \boldsymbol{\delta})$ is the power density consisting of a weighted sum of Laplace densities, which have standard deviations σ_{AS} corresponding to the angular spread of the propagation clusters. The specifications in [8] for channel simulations include an angular spread of $\sigma_{\text{AS}} = 2^\circ$ and $\sigma_{\text{AS}} = 5^\circ$ for the NLoS clusters in an urban macro and urban micro cell, respectively. For further details on the used spatial channel model, the reader is referred to [3]. This work considers the channel parameters to be constant within one coherence interval, i.e., $\boldsymbol{\delta}$ and θ do not change over the T observations. The channel covariance matrix of $\mathbf{h}(t)$ can then be written as

$$\mathbf{C}_{\delta, \theta} = \frac{KM}{K+1} \mathbf{a}(\theta) \mathbf{a}^H(\theta) + \frac{M}{K+1} \mathbf{C}_{\text{NLoS}}(\boldsymbol{\delta}). \quad (5)$$

If the BS employs a uniform linear array (ULA), the steering vector is given as

$$\mathbf{a}(\theta) = \frac{1}{\sqrt{M}} \left[1, e^{-j2\pi \frac{d}{\lambda} \sin(\theta)}, \dots, e^{-j2\pi \frac{d}{\lambda} (M-1) \sin(\theta)} \right]^T, \quad (6)$$

where d and λ are the antenna element spacing and the carrier frequency wavelength, respectively.

We estimate the most recent channel realization $\mathbf{h}(T)$, where we will drop the index from now on for notational convenience. Depending on the channel estimation method, we either infer the channel solely from the most recent observation $\mathbf{y}(T)$, or we utilize all observations $\mathbf{y}(t)$, $t = 1, \dots, T$. In the former case, we drop the index again for convenience.

III. PROPOSED METHOD

In order to utilize structural information given as additional prior information about the channel, we propose a DoA-aided two-stage approach, making the channel estimate more robust against noise. Given an observation \mathbf{y} and the DoA of the dominant path denoted by θ the MSE optimal estimator of \mathbf{h} , i.e., MMSE-achieving, is given by the conditional mean estimator (CME)

$$\hat{\mathbf{h}} = \mathbb{E}[\mathbf{h} | \mathbf{y}, \theta]. \quad (7)$$

To incorporate this prior information, we make use of a two-stage approach. Similarly to the GSC [13], we split the estimation problem into two parts. To this end, we rewrite the observation as

$$\tilde{\mathbf{y}} = \mathbf{T}^H(\theta) \mathbf{y} = \begin{bmatrix} \mathbf{a}^H(\theta) \\ \mathbf{V}^H(\theta) \end{bmatrix} \mathbf{y} = \begin{bmatrix} \tilde{y}_{\mathbf{a}} \\ \tilde{y}_{\tilde{\mathbf{a}}} \end{bmatrix} = \begin{bmatrix} \tilde{h}_{\mathbf{a}} \\ \tilde{h}_{\tilde{\mathbf{a}}} \end{bmatrix} + \mathbf{n}, \quad (8)$$

with $\mathbf{V}^H(\theta) \mathbf{a}(\theta) = \mathbf{0}$. Consequently, we can denote with $\mathbf{h}_{\mathbf{a}} = \mathbf{a}(\theta) \tilde{h}_{\mathbf{a}}$ and $\mathbf{h}_{\tilde{\mathbf{a}}} = \mathbf{V}(\theta) \tilde{h}_{\tilde{\mathbf{a}}}$ the parts of the channel along the dominant directions and in the subspace orthogonal to the dominant direction, respectively. In [14] two fast algorithms to find $\mathbf{V}(\theta)$ are described. If we choose the transformation $\mathbf{T}^H(\theta)$ as unitary, the statistics of the noise \mathbf{n} are not changed. As stated in [13], the MMSE is preserved for any full-rank transformation $\mathbf{T}^H(\theta)$. We can now formulate two independent estimators for each part via

$$\hat{h}_{\mathbf{a}} = \mathbf{a}(\theta) \mathbb{E}[\tilde{h}_{\mathbf{a}} | \tilde{y}_{\mathbf{a}}, \theta], \quad (9)$$

$$\hat{h}_{\tilde{\mathbf{a}}} = \mathbf{V}(\theta) \mathbb{E}[\tilde{h}_{\tilde{\mathbf{a}}} | \tilde{y}_{\tilde{\mathbf{a}}}, \theta], \quad (10)$$

The overall estimate is given as

$$\hat{\mathbf{h}} = \hat{h}_{\mathbf{a}} + \hat{h}_{\tilde{\mathbf{a}}}. \quad (11)$$

A. Estimation of Dominant Direction Component

The first entry of $\tilde{\mathbf{y}}$ defined in (8) is

$$\tilde{y}_{\mathbf{a}} = \mathbf{a}^H(\theta) \mathbf{h} + \mathbf{a}^H(\theta) \mathbf{n} = \tilde{h}_{\mathbf{a}} + \tilde{n}, \quad (12)$$

where $\tilde{h}_{\mathbf{a}}$ denotes the power of the channel along the steering vector $\mathbf{a}(\theta)$. Due to the absence of a closed-form optimal solution, we utilize a LMMSE estimator to obtain an estimate of $\mathbf{h}_{\mathbf{a}}$ via

$$\hat{h}_{\mathbf{a}, \text{LMMSE}} = \mathbf{a}(\theta) \frac{\mathbb{E} [|\tilde{h}_{\mathbf{a}}|^2]}{\mathbb{E} [|\tilde{h}_{\mathbf{a}}|^2] + \sigma^2} \tilde{y}_{\mathbf{a}} = \mathbf{a}(\theta) \frac{P_{\mathbf{a}}}{P_{\mathbf{a}} + \sigma^2} \tilde{y}_{\mathbf{a}}. \quad (13)$$

B. Estimation of Orthogonal Subspace Component

The CME for the second component given in (10) can not be calculated analytically, since the probability density functions

(PDFs) of the distributions are unknown. To this end, let us first observe the following

$$f_{\tilde{\mathbf{h}}_{\bar{a}}|\tilde{\mathbf{y}}_{\bar{a}},\theta}(\tilde{\mathbf{h}}_{\bar{a}}|\tilde{\mathbf{y}}_{\bar{a}},\theta) = \frac{f_{\tilde{\mathbf{y}}_{\bar{a}}|\tilde{\mathbf{h}}_{\bar{a}},\theta}(\tilde{\mathbf{y}}_{\bar{a}}|\tilde{\mathbf{h}}_{\bar{a}},\theta)f_{\tilde{\mathbf{h}}_{\bar{a}}|\theta}(\tilde{\mathbf{h}}_{\bar{a}}|\theta)}{f_{\tilde{\mathbf{y}}_{\bar{a}}|\theta}(\tilde{\mathbf{y}}_{\bar{a}}|\theta)} \quad (14)$$

$$= \frac{f_{\tilde{\mathbf{n}}}(\tilde{\mathbf{y}}_{\bar{a}} - \tilde{\mathbf{h}}_{\bar{a}})f_{\tilde{\mathbf{h}}_{\bar{a}}|\theta}(\tilde{\mathbf{h}}_{\bar{a}}|\theta)}{f_{\tilde{\mathbf{y}}_{\bar{a}}|\theta}(\tilde{\mathbf{y}}_{\bar{a}}|\theta)}. \quad (15)$$

If $f_{\tilde{\mathbf{h}}_{\bar{a}}|\theta}(\tilde{\mathbf{h}}_{\bar{a}}|\theta)$ and $f_{\tilde{\mathbf{y}}_{\bar{a}}|\theta}(\tilde{\mathbf{y}}_{\bar{a}}|\theta)$ are distributed following a GMM, a closed form solution for the CME $\mathbb{E}[\tilde{\mathbf{h}}_{\bar{a}}|\tilde{\mathbf{y}}_{\bar{a}},\theta]$ can be formulated, cf., [4].

To this end, we approximate the PDF of $\mathbf{h}_{\bar{a}}$ using a GMM motivated by their universal approximation property [4], [15]

$$f_{\mathbf{h}_{\bar{a}}}^{(J)}(\mathbf{h}_{\bar{a}}) = \sum_{j=1}^J p(j)\mathcal{N}_{\mathbb{C}}(\mathbf{h}_{\bar{a}}; \boldsymbol{\mu}_j, \mathbf{C}_j), \quad (16)$$

where $p(j)$, $\boldsymbol{\mu}_j$, and \mathbf{C}_j are the mixing coefficient, mean, and covariance matrix of the j -th GMM component, respectively. Let us further introduce the following approximation

$$\mathbf{h}_{\bar{a}} = (\mathbf{I} - \mathbf{a}(\theta)\mathbf{a}^H(\theta))\mathbf{h} \quad (17)$$

$$= \sqrt{\frac{M}{K+1}}\mathbf{h}_{\text{NLoS}} - \sqrt{\frac{M}{K+1}}\mathbf{a}(\theta)\mathbf{a}^H(\theta)\mathbf{h}_{\text{NLoS}} \quad (18)$$

$$\approx \sqrt{\frac{M}{K+1}}\mathbf{h}_{\text{NLoS}}, \quad (19)$$

where we essentially neglect the contribution of the second term in (18). This assumption is reasonable when the number of antennas is large enough [16]. Building on the approximation of $\mathbf{h}_{\bar{a}}$ in (19) and assuming that it is uncorrelated with the DoA θ , i.e., $\mathbf{h}_{\bar{a}}|\theta = \mathbf{h}_{\bar{a}}$, we can now obtain an expression for the conditional PDF of $\tilde{\mathbf{h}}_{\bar{a}}$ based on (16) as

$$f_{\tilde{\mathbf{h}}_{\bar{a}}|\theta}^{(J)}(\tilde{\mathbf{h}}_{\bar{a}}|\theta) = \sum_{j=1}^J p(j)\mathcal{N}_{\mathbb{C}}(\tilde{\mathbf{h}}_{\bar{a}}; \mathbf{V}(\theta)^H\boldsymbol{\mu}_j, \mathbf{V}(\theta)^H\mathbf{C}_j\mathbf{V}(\theta)), \quad (20)$$

which follows from the transformation $\mathbf{T}^H(\theta)$ in (8). The conditional PDF of the pilot observation $\tilde{\mathbf{y}}_{\bar{a}}$ can then be approximated by

$$f_{\tilde{\mathbf{y}}_{\bar{a}}|\theta}^{(J)}(\tilde{\mathbf{y}}_{\bar{a}}|\theta) = \sum_{j=1}^J p(j)\mathcal{N}_{\mathbb{C}}(\tilde{\mathbf{y}}_{\bar{a}}; \mathbf{V}(\theta)^H\boldsymbol{\mu}_j, \mathbf{V}(\theta)^H\mathbf{C}_j\mathbf{V}(\theta) + \mathbf{C}_{\tilde{\mathbf{n}}}). \quad (21)$$

Leveraging this found approximation of the conditional PDFs of $\tilde{\mathbf{h}}_{\bar{a}}$ and $\tilde{\mathbf{y}}_{\bar{a}}$, a convex combination of LMMSE estimates can be used to find the channel estimate in (10) [4]. As the covariance matrices of each component in (20) and (21) are calculated using the current DoA, we propose to utilize an alternative approach, which was introduced in [17], to reduce computational complexity. Here, instead of solving the estimation for $\tilde{\mathbf{h}}_{\bar{a}}$ we directly estimate $\mathbf{h}_{\bar{a}}$. This is done by taking the projection $\mathbf{y}_{\bar{a}} = \mathbf{V}(\theta)\mathbf{V}^H(\theta)\mathbf{y}$ as a preprocessing

step and consequently leaving the J LMMSE filters unaltered. Following a similar argumentation as in [17], we assume that the noise of the $\mathbf{y}_{\bar{a}}$ component is Gaussian with the covariance matrix $\mathbf{C}_{\tilde{\mathbf{n}}} = \sigma^2\frac{M-1}{M}\mathbf{I}_M$. The resulting estimator can be written as

$$\hat{\mathbf{h}}_{\bar{a},\text{GMM}} = \sum_{j=1}^J p(j|\mathbf{y}_{\bar{a}})\hat{\mathbf{h}}_{\bar{a},\text{GMM},j} \quad (22)$$

with

$$p(j|\mathbf{y}_{\bar{a}}) = \frac{p(j)\mathcal{N}_{\mathbb{C}}(\mathbf{y}_{\bar{a}}; \boldsymbol{\mu}_j, \mathbf{C}_j + \mathbf{C}_{\tilde{\mathbf{n}}})}{\sum_{i=1}^J p(i)\mathcal{N}_{\mathbb{C}}(\mathbf{y}_{\bar{a}}; \boldsymbol{\mu}_i, \mathbf{C}_i + \mathbf{C}_{\tilde{\mathbf{n}}})} \quad (23)$$

and

$$\hat{\mathbf{h}}_{\bar{a},\text{GMM},j} = \mathbf{C}_j(\mathbf{C}_j + \mathbf{C}_{\tilde{\mathbf{n}}})^{-1}(\mathbf{y}_{\bar{a}} - \boldsymbol{\mu}_j) + \boldsymbol{\mu}_j. \quad (24)$$

As our simulations did not show any significant difference between the estimator based on (20) and (21) and the computational more efficient estimator formulated in (22)-(24), we will focus in the following on the latter, due to better complexity.

C. Augmentation of Training Data

In order to approximate the proposed estimators based on a representative training set $\mathcal{H} = \{\mathbf{h}_{\ell}\}_{\ell=1}^L$ of L samples, the following augmentation is done. First, we determine the DoA θ_{ℓ} of each channel realization \mathbf{h}_{ℓ} within the training set \mathcal{H} as

$$\theta_{\ell} = \arg \max_{\theta \in \Theta} |\mathbf{a}^H(\theta)\mathbf{h}_{\ell}|, \quad (25)$$

where Θ defines the set of possible angles. Sequentially, we construct two sets $\mathcal{H}_{\mathbf{a}} = \{\mathbf{h}_{\mathbf{a},\ell}\}_{\ell=1}^L$ and $\mathcal{H}_{\bar{\mathbf{a}}} = \{\mathbf{h}_{\bar{\mathbf{a}},\ell}\}_{\ell=1}^L$, where we project each channel sample \mathbf{h}_{ℓ} using the transformation $\mathbf{T}(\theta_{\ell})$. This is done with

$$\tilde{\mathbf{h}}_{\mathbf{a},\ell} = \mathbf{a}^H(\theta_{\ell})\mathbf{h}_{\ell} \quad (26)$$

and

$$\mathbf{h}_{\bar{\mathbf{a}},\ell} = \mathbf{V}(\theta_{\ell})\mathbf{V}^H(\theta_{\ell})\mathbf{h}_{\ell} = (\mathbf{I}_M - \mathbf{a}(\theta_{\ell})\mathbf{a}^H(\theta_{\ell}))\mathbf{h}_{\ell}, \quad (27)$$

where θ_{ℓ} is provided by (25). Based on the training set $\mathcal{H}_{\mathbf{a}}$ we can estimate $\hat{P}_{\mathbf{a}} = 1/L \sum_{\ell=1}^L |\tilde{\mathbf{h}}_{\mathbf{a},\ell}|^2$ in (13) and given $\mathcal{H}_{\bar{\mathbf{a}}}$, the fitting of the components in (16) is done with the well-known expectation-maximization (EM) algorithm [18].

D. DoA Estimation

The transformation $\mathbf{T}(\theta)$ in (8) is based on the DoA of the LoS path. As in practice, the true angle is not given, we approximate the transform with

$$\mathbf{T}(\theta) \approx \mathbf{T}(\hat{\theta}), \quad (28)$$

where $\hat{\theta}$ denotes the DoA estimate. In a JCAS setup, the DoA estimate or the user's position might be given by other system functionalities, e.g., radar. Since this assumption may not always be fulfilled, especially regarding systems not directly built for JCAS, the DoA estimation may need to be conducted while estimating the channel. We want to emphasize, that our proposed approach is independent of the used DoA estimation algorithm, e.g., the well-known multiple signal classification

(MUSIC) algorithm [19], root-MUSIC [20] and estimation of signal parameters via rotational invariance techniques (ESPRIT) [21]. Additionally, as the DoAs do not change rapidly, computational efficient tracking algorithms, which either track the subspace [22], [23] or the DoA [24], can be utilized.

IV. BASELINE ESTIMATORS

The conventional least squares (LS) channel estimator is given as $\hat{\mathbf{h}}_{\text{LS}} = \mathbf{y}$. Furthermore, the GMM estimator from [4] can be used to estimate the whole channel by fitting the GMM onto the representative data set $\mathcal{H} = \{\mathbf{h}_\ell\}_{\ell=1}^L$ and inferring the estimate $\hat{\mathbf{h}}_{\text{GMM}}$.

The orthogonal matching pursuit (OMP) [25] is a well-known example from the field of compressed sensing (CS). Since it needs to know the sparsity order, we evaluate a genie-aided variant (“genieOMP”), where OMP chooses the optimal sparsity order based on the true channel \mathbf{h} .

Purely parametric channel estimation schemes, e.g., [5], assume a ray-based channel model as $\mathbf{h} \approx \mathbf{A}(\boldsymbol{\theta})\mathbf{s}$, where $\mathbf{A}(\boldsymbol{\theta}) = [\mathbf{a}(\theta_1), \dots, \mathbf{a}(\theta_P)] \in \mathbb{C}^{M \times P}$ is the steering matrix of the P paths and \mathbf{s} holds the complex path gains. For a given set of estimated DoAs $\hat{\boldsymbol{\theta}}$, the LS solution can be found as

$$\hat{\mathbf{h}}_{\text{para}} = \mathbf{A}(\hat{\boldsymbol{\theta}}) \left(\mathbf{A}^H(\hat{\boldsymbol{\theta}})\mathbf{A}(\hat{\boldsymbol{\theta}}) \right)^{-1} \mathbf{A}^H(\hat{\boldsymbol{\theta}})\mathbf{y}. \quad (29)$$

Similar to [5], we implement forward-backward averaging for the ESPRIT algorithm to enhance its estimation quality. As the number of paths needs to be known, we again implement genie-aided variants, where the number of paths is chosen based on the true channel \mathbf{h} .

Another estimator is based on the global sample covariance matrix, which we can compute from the training data set $\mathcal{H}_{\bar{\mathbf{a}}}$ with $\mathbf{C}_{\bar{\mathbf{a}}} = 1/L \sum_{\mathbf{h}_{\bar{\mathbf{a}}} \in \mathcal{H}_{\bar{\mathbf{a}}}} \mathbf{h}_{\bar{\mathbf{a}}}\mathbf{h}_{\bar{\mathbf{a}}}^H$. We can use this sample covariance matrix to formulate the LMMSE estimator for the NLoS components as

$$\hat{\mathbf{h}}_{\bar{\mathbf{a}},\text{s-cov}} = \mathbf{C}_{\bar{\mathbf{a}}} \left(\mathbf{C}_{\bar{\mathbf{a}}} + \sigma^2 \frac{M-1}{M} \mathbf{I}_M \right)^{-1} \mathbf{P}_{\bar{\mathbf{a}}}\mathbf{y}. \quad (30)$$

The LoS component is estimated as in (13).

When working with the channel model described in Section II, the true conditional covariance matrix $\mathbf{C}_{\delta,\theta}$ of every channel realization is known, and we can construct the utopian genie LMMSE estimator as

$$\hat{\mathbf{h}}_{\text{genieLMMSE}} = \mathbf{C}_{\delta,\theta} \left(\mathbf{C}_{\delta,\theta} + \sigma^2 \mathbf{I}_M \right)^{-1} \mathbf{y}. \quad (31)$$

V. NUMERICAL SIMULATIONS

In this work, we consider a base station that serves a sector of 120° , i.e., the angle of the LoS path is drawn uniformly in the interval $[-60^\circ, 60^\circ]$. We normalize the channel realizations with $\mathbb{E}[\|\mathbf{h}\|^2] = M$ such that we can define the signal-to-noise ratio (SNR) $= \frac{1}{\sigma^2}$. Given N channel estimates $\{\hat{\mathbf{h}}_n\}_{n=1}^N$ of the test samples $\{\mathbf{h}_n\}_{n=1}^N$, we can define the normalized MSE (MSE) as $\frac{1}{NM} \sum_{n=1}^N \|\mathbf{h}_n - \hat{\mathbf{h}}_n\|^2$. The simulations are carried out $N = 10^3$ times. We use $T = 10$ observation for each covariance coherence interval if not stated otherwise. The number of BS antennas is $M = 64$ with an antenna spacing

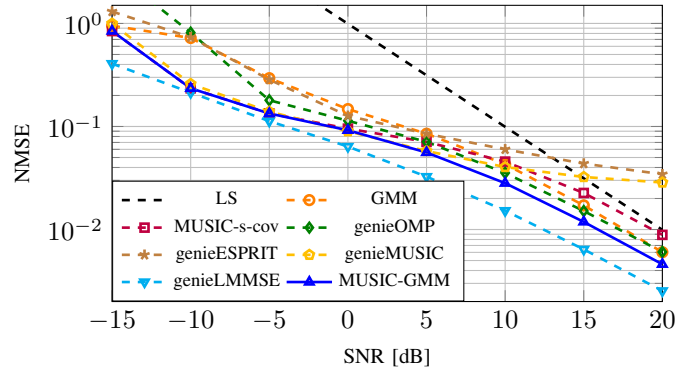


Fig. 2. NMSE for given channel estimations based on $T = 10$ pilot observations. The angular spread of the NLoS clusters set to $\sigma_{\text{AS}} = 2^\circ$ and the Rician factor is $K = 10$ dB.

of $d = \lambda/2$. We simulate three NLoS propagation clusters, assuming an angular spread of $\sigma_{\text{AS}} = 2^\circ$ in accordance to [8], if not stated otherwise. The NLoS channel realizations are then constructed according to [3]. We use $1.5 \cdot 10^5$ training samples to fit a GMM with $J = 128$ components for each scenario, where we use a grid Θ with $16M$ points to estimate the DoA. For the first stage of the proposed method, we use MUSIC, with the same grid size. To this end, we take the last T observations and construct the sample covariance matrix

$$\hat{\mathbf{C}}_{\mathbf{y}} = \frac{1}{T} \mathbf{Y} \mathbf{Y}^H, \quad (32)$$

where $\mathbf{Y} = [\mathbf{y}(1), \dots, \mathbf{y}(T)] \in \mathbb{C}^{M \times T}$. Based on $\hat{\mathbf{C}}_{\mathbf{y}}$, we calculate the DoA estimate $\hat{\boldsymbol{\theta}}$. The resulting estimator is denoted as “MUSIC-GMM”. The “MUSIC-s-cov” estimator utilizes the same training samples.

In Fig. 2, the performance for a Rician factor of $K = 10$ dB is shown for different SNR. We can observe that in the low SNR regime, the three methods based on MUSIC perform the best, even approaching the “genieLMMSE”. For this low SNR region, the estimation of the LoS component dominates the problem and, hence, all MUSIC-based estimators perform similar. For high SNR values, estimating the NLoS clusters is important. Here, our proposed “MUSIC-GMM” estimator performs extraordinarily well. Furthermore, the parametric channel estimators saturate for high SNR due to their model mismatch.

Since the channel characteristics depend heavily on the Rician factor K , Fig. 3 shows the performance for different Rician factors. All considered estimators show increasing performance with an increase of the Rician factor. This is because estimating the NLoS components becomes less significant. Although “genieOMP” and “genieMUSIC” utilize genie knowledge, our proposed channel estimation method exhibits at least a comparable performance for the different Rician factors.

Fig. 4 shows the dependency of the performance on the angular spread σ_{AS} of the NLoS clusters. As σ_{AS} increases, the parametric and sparse channel estimators degrade in their performance. The angular spread for a typical sub 6 GHz scenario is specified in [8] as $\sigma_{\text{AS}} = 2^\circ$ and $\sigma_{\text{AS}} = 5^\circ$ for urban macro and urban micro cells, respectively. With increasing

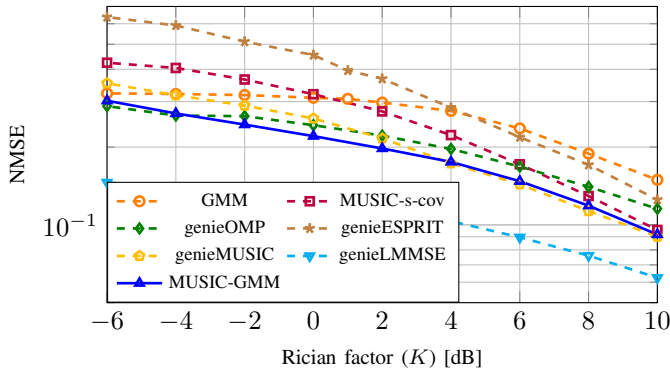


Fig. 3. NMSE for given channel estimations based on $T = 10$ pilot observations at SNR = 0 dB. The angular spread of the NLoS clusters is set to $\sigma_{AS} = 2^\circ$.

angular spread σ_{AS} , our proposed method exhibits a smaller gap to the utopian “genieLMMSE” and outperforms all of the other baselines for $\sigma_{AS} \geq 2^\circ$.

VI. CONCLUSION

In this work, we proposed a DoA-aided MMSE-based channel estimation. To this end, we first introduced a DoA-based reformulation of the observations similar to GSC. Two independent estimators are introduced, where the NLoS clusters are estimated utilizing the GMM framework from [4]. Extensive simulations showed superior performance of our proposed estimation approach compared to state-of-the-art baselines in the considered realistic scenarios. Further evaluations with real-world measurements are planned for future work. Additionally, we intend to investigate further applications, including coarsely quantized systems and the movement of UEs along trajectories.

REFERENCES

- [1] F. Rusek, D. Persson, B. K. Lau, E. G. Larsson, T. L. Marzetta, O. Edfors, and F. Tufvesson, “Scaling up MIMO: Opportunities and challenges with very large arrays,” *IEEE Signal Processing Magazine*, vol. 30, no. 1, pp. 40–60, 2013.
- [2] M. Soltani, V. Pourahmadi, A. Mirzaei, and H. Sheikhzadeh, “Deep learning-based channel estimation,” *IEEE Communications Letters*, vol. 23, no. 4, pp. 652–655, 2019.
- [3] D. Neumann, T. Wiese, and W. Utschick, “Learning the MMSE channel estimator,” *IEEE Transactions on Signal Processing*, vol. 66, no. 11, pp. 2905–2917, 2018.
- [4] M. Koller, B. Fesl, N. Turan, and W. Utschick, “An asymptotically MSE-optimal estimator based on Gaussian mixture models,” *IEEE Transactions on Signal Processing*, vol. 70, pp. 4109–4123, 2022.
- [5] R. Shafin, L. Liu, J. Zhang, and Y.-C. Wu, “DoA estimation and capacity analysis for 3-d millimeter wave massive-MIMO/FD-MIMO OFDM systems,” *IEEE Transactions on Wireless Communications*, vol. 15, no. 10, pp. 6963–6978, 2016.
- [6] M. D. Larsen, A. L. Swindlehurst, and T. Svantesson, “Performance bounds for MIMO-OFDM channel estimation,” *IEEE Transactions on Signal Processing*, vol. 57, no. 5, pp. 1901–1916, 2009.
- [7] F. Liu, Y. Cui, C. Masouros, J. Xu, T. X. Han, Y. C. Eldar, and S. Buzzi, “Integrated sensing and communications: Toward dual-functional wireless networks for 6G and beyond,” *IEEE Journal on Selected Areas in Communications*, vol. 40, no. 6, pp. 1728–1767, 2022.
- [8] 3GPP, “Spatial channel model for multiple input multiple output (MIMO) simulations,” 3rd Generation Partnership Project (3GPP), Tech. Rep. 25.996 v16.0.0, 2020.

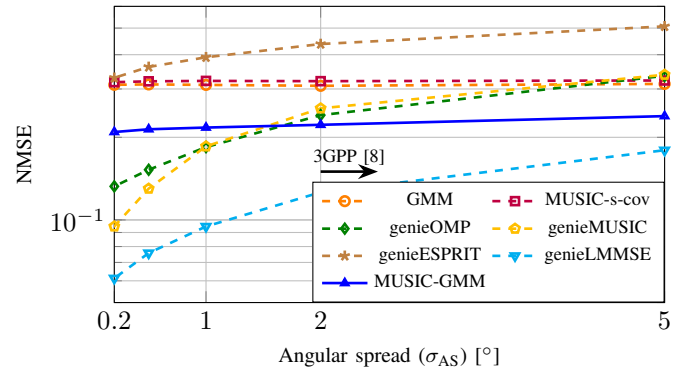


Fig. 4. NMSE for given channel estimations based on $T = 10$ pilot observations at SNR = 0 dB and $K = 0$ dB.

- [9] B. Antonescu, M. T. Moayyed, and S. Basagni, “Diffuse scattering models for mmwave V2X communications in urban scenarios,” in *2019 International Conf. on Computing, Networking and Communications (ICNC)*, 2019, pp. 923–929.
- [10] D. Tse and P. Viswanath, *Fundamentals of Wireless Communication*. Cambridge University Press, 2005.
- [11] H. Yin, D. Gesbert, M. Filippou, and Y. Liu, “A coordinated approach to channel estimation in large-scale multiple-antenna systems,” *IEEE Journal on Selected Areas in Communications*, vol. 31, no. 2, pp. 264–273, 2013.
- [12] Ö. Özdogan, E. Björnson, and J. Zhang, “Performance of cell-free massive MIMO with Rician fading and phase shifts,” *IEEE Transactions on Wireless Communications*, vol. 18, no. 11, pp. 5299–5315, 2019.
- [13] L. Griffiths and C. Jim, “An alternative approach to linearly constrained adaptive beamforming,” *IEEE Transactions on Antennas and Propagation*, vol. 30, no. 1, pp. 27–34, 1982.
- [14] J. Goldstein and I. Reed, “Theory of partially adaptive radar,” *IEEE Transactions on Aerospace and Electronic Systems*, vol. 33, no. 4, pp. 1309–1325, 1997.
- [15] T. T. Nguyen, H. D. Nguyen, F. Chamroukhi, and G. J. McLachlan, “Approximation by finite mixtures of continuous density functions that vanish at infinity,” *Cogent Mathematics & Statistics*, vol. 7, no. 1, p. 1750861, 2020.
- [16] E. Björnson, J. Hoydis, and L. Sanguinetti, “Massive MIMO networks: Spectral, energy, and hardware efficiency,” *Foundations and Trends® in Signal Processing*, vol. 11, no. 3-4, pp. 154–655, 2017.
- [17] F. Weißer, N. Turan, D. Semmler, and W. Utschick, “Data-aided channel estimation utilizing Gaussian mixture models,” in *2024 IEEE International Conf. on Acoustics, Speech and Signal Processing (ICASSP)*, 2024.
- [18] C. M. Bishop, *Pattern Recognition and Machine Learning (Information Science and Statistics)*. Berlin, Heidelberg: Springer-Verlag, 2006.
- [19] R. Schmidt, “Multiple emitter location and signal parameter estimation,” *IEEE Transactions on Antennas and Propagation*, vol. 34, no. 3, pp. 276–280, 1986.
- [20] A. Barabell, “Improving the resolution performance of eigenstructure-based direction-finding algorithms,” in *ICASSP ’83. IEEE International Conf. on Acoustics, Speech, and Signal Processing*, vol. 8, 1983, pp. 336–339.
- [21] R. Roy and T. Kailath, “ESPRIT-estimation of signal parameters via rotational invariance techniques,” *IEEE Transactions on Acoustics, Speech, and Signal Processing*, vol. 37, no. 7, pp. 984–995, 1989.
- [22] B. Yang, “Projection approximation subspace tracking,” *IEEE Transactions on Signal Processing*, vol. 43, no. 1, pp. 95–107, 1995.
- [23] W. Utschick, “Tracking of signal subspace projectors,” *IEEE Transactions on Signal Processing*, vol. 50, no. 4, pp. 769–778, 2002.
- [24] C. Sastry, E. Kamen, and M. Simaan, “An efficient algorithm for tracking the angles of arrival of moving targets,” *IEEE Transactions on Signal Processing*, vol. 39, no. 1, pp. 242–246, 1991.
- [25] Y. Pati, R. Rezaifar, and P. Krishnaprasad, “Orthogonal matching pursuit: recursive function approximation with applications to wavelet decomposition,” in *Proceedings of 27th Asilomar Conf. on Signals, Systems and Computers*, 1993, pp. 40–44 vol.1.